ELSEVIER

Biophysical Chemistry 99 (2002) 259–270

Biophysical Chemistry

www.elsevier.com/locate/bpc

Simulations of temperature sensitivity of the peroxidase–oxidase oscillator

Kirsten Rosendal Valeur*, Robert degli Agosti

Department of Plant Biology and Biochemistry, University of Geneva, 3 Place de l'Université, CH-1211 Geneva 4, Switzerland

Received 6 May 2002; received in revised form 17 June 2002; accepted 17 June 2002

Abstract

The influence of temperature on the oscillatory kinetics of the peroxidase–oxidase reaction was studied theoretically. Assuming $Q_{10}=2$ for elementary reactions, the effect of multiplying the rate constants of the model by factors between 0.5 and 2 (corresponding to a 10 °C decrease and increase, respectively, of temperature) was investigated. First, the individual rate constants were successively multiplied by 0.5 or 2 while all other rate constants were kept unchanged. This resulted in either a longer or a shorter period, depending on the rate constant being changed. Multiplication by 0.5 or by 2 generally resulted in opposite effects on the period length. However, the absolute value of this deviation differed. Also, the dynamics changed when halving the dimerization rate of $NAD^{\bullet}$ as well as when doubling the rate constant for the reduction of ferric peroxidase by $NAD^{\bullet}$. Next, simulations were performed multiplying all rate constants by one and the same factor, which increased progressively from 0.5 to 2. Intervals were found corresponding to temperature dependency, compensation, and over-compensation, respectively.

Keywords: Peroxidase–oxidase; Temperature compensation; Model; Simulation; Oscillation

1. Introduction

Peroxidase is a heme protein, which in its native form has iron in the ferric state (Fe^{3+}) and is designated per^{3+}. The protein can have other redox states, classified in accordance with the oxidation state of the heme iron: ferrous peroxidase (per^{2+}), compound I (coI), compound II (coII), and compound III (coIII). The compounds have the oxidation states 5+, 4+ and 6+, respectively. Horseradish peroxidase (HRP) catalyzes the reduction of hydrogen peroxide in the presence of one of a very large number of different hydrogen donors [1]. In addition to this reaction, HRP catalyzes the peroxidase–oxidase (PO) reaction, in which molecular oxygen is the electron acceptor. For this reaction, fewer hydrogen donors are known, such as reduced nicotinamide adenine dinucleotide (NADH) [2]. Using this substrate in an open in vitro system, oscillatory kinetics could be observed [3,4]. The study of the PO reaction in vivo [5] so far has not led to observation of oscillatory kinetics. It has been proposed that if oscillatory dynamics do exist in vivo, the advan-

*Corresponding author. Combio A/S, Gamle Carlsberg Vej 10, DK-2500 Valby, Copenhagen, Denmark. Tel.: +45-33-27-52-57; fax: +45-33-27-53-71.

E-mail address: krv@combio.dk (K.R. Valeur).

0301-4622/02/$ - see front matter © 2002 Elsevier Science B.V. All rights reserved.
PII: S0301-4622(02)00226-0

tageous effect of this could be maintaining a low average level of the involved toxic, free radicals [6].

Besides sustained oscillations [7], the PO reaction exhibits other non-linear dynamics, such as bistability [8], mixed-mode oscillations [9], and chaos [10,11]. In order to simulate these different non-linear dynamics, several models have been proposed. These can be divided into two categories: simple abstract models, and detailed models.

The abstract models consider the essential features of the reaction rather than the individual steps and attempt to account for the observed nonlinear dynamics. Using a four-variable model composed of two coupled autocatalytic cycles, periodic and chaotic dynamics were simulated [12].

Several more detailed models of the PO reaction, which include the principal reaction steps, have been proposed. They are based on the so-called YY model [13]. The first models omitted per^{2+}, as ferrous peroxidase is present only in small amounts in the PO reaction catalyzed by HRP. However, its inclusion allowed for chaotic dynamics to occur [14]. With these first detailed models some experimental behavior could be simulated qualitatively. Their insufficiency is due to incomplete reaction schemes and a lack of experimentally founded values. Two recent models, which use chemically realistic values, are the Urbanalator model [15] and the BFSO model [16].

The Urbanalator model omits ferrous peroxidase, as Olson et al. [15] did not observe this enzyme intermediate experimentally. Their model includes NADH decay due to illumination from the deuterium lamp of the spectrophotometer [17]. Also, autoxidation of NADH with the formation of H_2O_2 was for the first time included in this model. Using chemically realistic rate constants from literature, simple oscillations of the concentrations of NADH, oxygen, per^{3+} and coIII could be simulated [15].

The BFSO model [16] is based on the Urbanalator model and experiments performed by Geest et al. [11]. Unlike the Urbanalator model, per^{2+} is included in this model. Its inclusion adds to the complexity of the system [14] and permitted to simulate the oscillatory kinetics using *Coprinus* peroxidase as a catalyst [18]. There are some discrepancies among these two models due to different values of rate constants found in literature and to differences in the extrapolations made to fit reported data with the experimental conditions of the PO oscillator. Using the BFSO model, not only simple oscillations can be simulated, but also experimentally observed complex behavior such as period doubling, chaos, and bistability [16].

Temperature compensation is a characteristic of most circadian systems [19] and was found also for some ultradian oscillators [20–23]. The phenomenon has been widely studied and remains a challenging topic. While a rise of temperature will accelerate elementary reactions, its influence on a reaction network system is more complex and can give rise to a variety of effects. The effect of this environmental parameter on a network system has been investigated theoretically [24–27].

Here, the influence of temperature on the PO network system is examined theoretically using the BFSO model [16]. The rate constants of the involved partial reactions are modified either individually or all together to simulate temperature changes, according to the procedure of Leloup and Goldbeter [28].

We provide evidence that the reaction is capable of exhibiting temperature dependency, as well as temperature compensation and over-compensation, depending on the temperature range considered.

2. The model

The present simulations are based on the BFSO model. Its reaction scheme is shown in Fig. 1. The equations are listed in Table 1 together with the rate constant values chosen for the present study. The background for the choices is described in the following.

The rate constants k_1–k_{11} are based on published general kinetic studies and adjusted to the experimental standard conditions for the PO oscillator, such as a temperature of 28 °C. The rate constant k_1 has been determined experimentally at pH 9 [29] and extrapolations made for conditions of the PO oscillator [15], assuming that the NADH oxidation is first order dependent on $[H^+]$, giving $k_1 = 33 \times 10^{-6}\ \mu M^{-1}\, s^{-1}$. Should this not be the

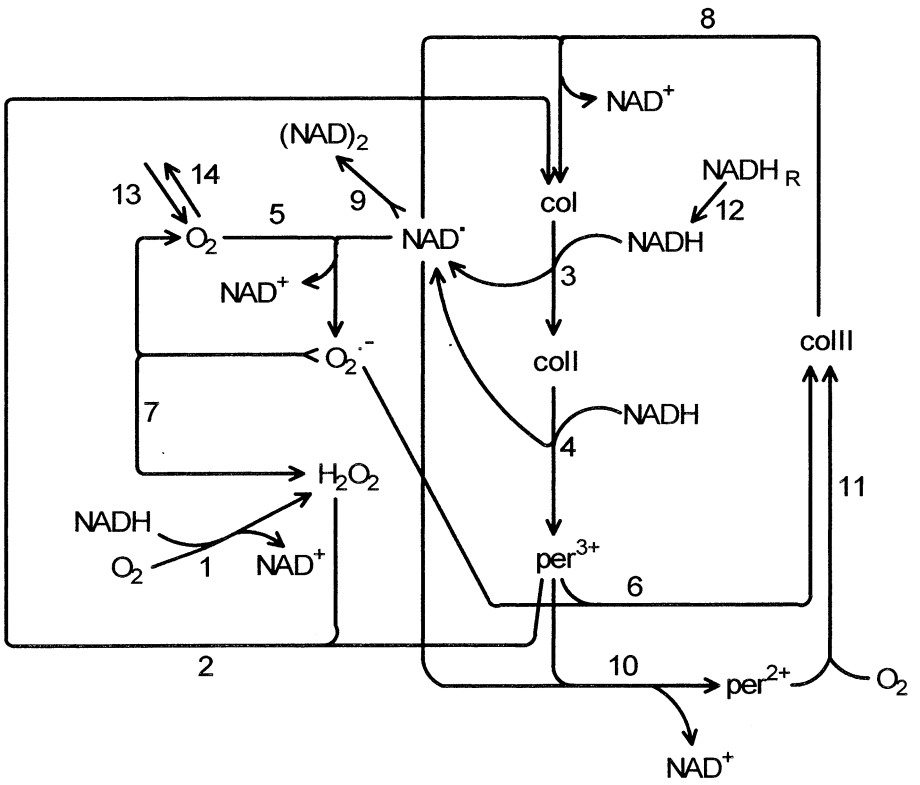

Fig. 1. Scheme of the BFSO model used for the present simulations. The reaction solution contains peroxidase, which is fed with a continuous inflow of the two substrates NADH (R_{12}) and oxygen (R_{13}). NADH slowly autoxidizes (R_1), thus providing the H_2O_2 necessary for initiating the classical peroxidasic cycle (R_2–R_4). In reactions R_3 and R_4, NADH is oxidized to the free radical NAD•, which reacts with oxygen to form superoxide (R_5). Superoxide will either dismutate to hydrogen peroxide (R_7) for use in the peroxidasic cycle, or it will be incorporated in the native peroxidase to form coIII (R_6). coIII is a rather inactive enzyme intermediate, which is decomposed to coI by reaction with NAD• (R_8). coI is reduced to the native per^{3+} in two steps (R_3–R_4). coIII can also be formed when per^{3+} is reduced to per^{2+} by NAD• (R_{10}) and per^{2+} reacts with molecular oxygen (R_{11}). For this second cycle, which has R_3 and R_4 in common with the peroxidasic cycle, oxygen is the electron acceptor (R_6 and R_{11}) instead of H_2O_2 (R_2), making the total reaction network a PO reaction.

case the value will be smaller at the standard pH value of the PO oscillator (pH 5.1). Simulations therefore have been performed with $k_1 = 3\times10^{-6}-9\times10^{-6}$ $\mu M^{-1}\,s^{-1}$ [16,18,30,31]. Here, the value of k_1 has been chosen as 6×10^{-6} $\mu M^{-1}\,s^{-1}$.

The rate constants k_2–k_7 are identical to values chosen for earlier simulations [16,18,30,31].

No experimental data are available for the rate constant of reaction R_8. Yokota and Yamazaki [13] simulated non-oscillatory kinetics observed at pH 5.6 setting the value of this rate constant at 130 $\mu M^{-1}\,s^{-1}$. Others have chosen values for k_8 between 60 and 150 $\mu M^{-1}\,s^{-1}$ [15,16,18,30,31]. Here, $k_8 = 100$ $\mu M^{-1}\,s^{-1}$ has been chosen.

The dimerization rate of NAD• radicals (k_9) was determined as 56 $\mu M^{-1}\,s^{-1}$ [32] and 77 ± 8 $\mu M^{-1}\,s^{-1}$ [33]. Here, $k_9 = 90$ $\mu M^{-1}\,s^{-1}$ was chosen.

Rate constants for the reactions involving ferrous peroxidase (R_{10} and R_{11}) have values identical with the BFSO model [16].

Rate constants k_{12}–k_{14} were based on experimental conditions for the PO oscillator (28 °C). The constants k_{13}–k_{14} relate to the transfer of oxygen into the solution (k_{13}) and its evaporation

Table 1
Equations from the BFSO model, chosen rate constants and initial concentrations, for the simulations

Model equation	Rate constant
(1) $NADH + O_2 + H^+ \rightarrow NAD^+ + H_2O_2$	$6\times10^{-6}\ \mu M^{-1}\ s^{-1}$
(2) $H_2O_2 + per^{3+} \rightarrow coI$	$18\ \mu M^{-1}\ s^{-1}$
(3) $CoI + NADH \rightarrow coII + NAD^{\bullet}$	$0.04\ \mu M^{-1}\ s^{-1}$
(4) $CoII + NADH \rightarrow per^{3+} + NAD^{\bullet}$	$0.026\ \mu M^{-1}\ s^{-1}$
(5) $O_2 + NAD^{\bullet} \rightarrow O_2^- + NAD^+$	$20\ \mu M^{-1}\ s^{-1}$
(6) $O_2^- + per^{3+} \rightarrow coIII$	$17\ \mu M^{-1}\ s^{-1}$
(7) $2\ O_2^- + 2\ H^+ \rightarrow H_2O_2 + O_2$	$20\ \mu M^{-1}\ s^{-1}$
(8) $CoIII + NAD^{\bullet} \rightarrow coI + NAD^+$	$100\ \mu M^{-1}\ s^{-1}$
(9) $2\ NAD^{\bullet} \rightarrow (NAD)_2$	$90\ \mu M^{-1}\ s^{-1}$
(10) $Per^{3+} + NAD^{\bullet} \rightarrow per^{2+} + NAD^+$	$1.8\ \mu M^{-1}\ s^{-1}$
(11) $Per^{2+} + O_2 \rightarrow coIII$	$0.1\ \mu M^{-1}\ s^{-1}$
(12) $NADH_R \rightarrow NADH$	$0.08\ \mu M\ s^{-1}$
(13) $O_{2(gas)} \rightarrow O_{2(liquid)}$	$0.04778\ \mu M\ s^{-1}$
(14) $O_{2(liquid)} \rightarrow O_{2(gas)}$	$0.0043\ s^{-1}$
Species[a]	**Initial concentration**
P_0 (HRP_0)	$1\ \mu M$
O_0 ($O_{2(0),aq}$)	$11.555\ \mu M$
Differential equations	
$[NADH]' = -k_1[NADH][O_2] - k_3[NADH][coI] - k_4[NADH][coII] + k_{12}$	
$[O_2]' = -k_1[NADH][O_2] - k_5[O_2][NAD^{\bullet}] + k_7[O_2^-][O_2^-] - k_{11}[per^{2+}][O_2] + k_{13} - k_{14}[O_2]$	
$[per^{3+}]' = -k_2[H_2O_2][per^{3+}] + k_4[NADH][coII] - k_6[per^{3+}][O_2^-] - k_{10}[per^{3+}][NAD^{\bullet}]$	
$[per^{2+}]' = k_{10}[per^{3+}][NAD^{\bullet}] - k_{11}[per^{2+}][O_2]$	
$[NAD^{\bullet}]' = k_3[NADH][coI] + k_4[NADH][coII] - k_5[O_2][NAD^{\bullet}] - k_8[coIII][NAD^{\bullet}] - 2\times k_9[NAD^{\bullet}][NAD^{\bullet}] - k_{10}[per^{3+}][NAD^{\bullet}]$	
$[O_2^-]' = k_5[O_2][NAD^{\bullet}] - k_6[per^{3+}][O_2^-] - 2\times k_7[O_2^-][O_2^-]$	
$[coI]' = k_2[H_2O_2][per^{3+}] - k_3[NADH][coI] + k_8[coIII][NAD^{\bullet}]$	
$[coII]' = k_3[NADH][coI] - k_4[NADH][coII]$	
$[coIII]' = k_6[O_2^-][per^{3+}] - k_8[coIII][NAD^{\bullet}] + k_{11}[per^{2+}][O_2]$	
$[H_2O_2]' = k_1[NADH][O_2] - k_2[H_2O_2][per^{3+}] + k_7[O_2^-][O_2^-]$	

The values of the rate constants correspond to standard conditions, 28 °C.
[a] For all other species the initial concentration is set at 0 μM.

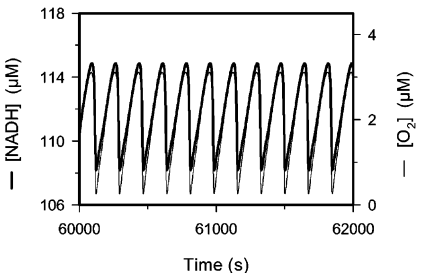

Fig. 2. Standard simulation using parameter values corresponding to 28 °C. Time series for NADH and oxygen.

(k_{14}) (e.g. [9,17]). The gas transfer constant k_{14} was determined as 0.0043 s^{-1}. Isolation of k_{13} in the equilibrium equation gives $k_{13}=0.04778$ $\mu M\ s^{-1}$.

The initial concentration of native peroxidase (per^{3+}) is set at 1 μM. No NADH is present in the beginning; the reaction starts with its continuous supply into the system. The initial steady state concentration of oxygen was calculated from tables of absorption coefficient, vapor pressure, salinity, and temperature [34,35] at standard conditions of 28 °C in 0.1 M acetate buffer as 11.555 μM. The initial concentrations of all other species were set at zero.

The values were changed in order to simulate oscillatory kinetics at other temperatures. The value of Q typically is close to 2 [36], i.e. the reaction rate is doubled for each 10 °C temperature increment and is halved for each 10 °C temperature diminution. Simulations therefore were performed multiplying the rate constants by 0.5 (corresponding to 18 °C), by 2.0 (corresponding to 38 °C), or by a factor in between. This does not apply to the NADH infusion rate (k_{12}), which is kept unchanged, neither to the oxygen transfer constants. k_{14} was determined experimentally at 20 °C (0.0039 s^{-1}) and 40 °C (0.0053 s^{-1}), and values for other temperatures were linearly extra or intrapolated. The initial oxygen concentration at different temperatures was calculated between 18 and 38 °C. For values between integer degrees Celsius, a linear approximation was made.

Simulations were performed using the LSODE implementation of the Gear's algorithm for stiff ordinary differential equations (LSODE, Livermore solver for ordinary differential equations) [37]. The integrator works in double precision, while the output file is single precision. Data were sampled once a second.

The results obtained by the integration method employed were compared to the results obtained with two other variable-stepsize methods, provided with the program Berkeley Madonna (www.berkeleymadonna.com): the Rosenbrock (stiff) method and the Auto-stepsize method.

3. Results

3.1. Standard simulation

Time series of NADH and oxygen for a standard simulation corresponding to 28 °C is shown in Fig. 2. Values for period as well as levels and amplitudes of concentrations of substrates and the enzyme intermediates per^{3+}, coIII, and per^{2+}, were compared with experimental data based on deconvoluted absorption spectra [6,38,39]. The period is 172 s, which was confirmed by the two integration methods Rosenbrock and Auto-stepsize. This is within the experimental range (140–180 s). The NADH concentration level using the three integration methods was found as 111.505 μM, which is somewhat above the experimental levels (35–98 μM), but its amplitude of 6.668 μM (Rosenbrock and Auto-stepsize: 6.669 μM) is within the experimental range (0.8–11 μM). Oxygen concentration has a level of 1.683 μM (Rosenbrock and Auto-stepsize: 1.681 μM) and an amplitude of 2.848 μM, which are slightly lower than the experimental results (2–5 μM and 3.5–5 μM, respectively). The level of per^{3+} (0.58 μM) is within the experimental range (0.4–1.3 μM) while its amplitude (0.38 μM) is lower (0.9–1.9). The level (0.32 μM) and amplitude (0.52 μM) of coIII are lower than the published results (0.55–1.2 μM and 0.7–1.4 μM, respectively), the per^{2+} level (0.08 μM) is within the range (0.04–0.1 μM) while its amplitude (0.15 μM) is higher ($\approx$0.08 μM). Based on this comparative study the simulated results are considered as being reasonably close to experimental conditions.

3.2. Successive multiplication of each constant by 0.5 or 2.0

In order to investigate the sensitivity of the whole network towards each constant with respect to a temperature change, simulations were performed multiplying the rate constants, one by one, successively (except k_{13} and k_{14}) by 0.5 or 2.0 while the other constants were kept unchanged. As in the case of choosing rate constants for the standard simulation, the rate constants for oxygen influx (k_{13}) and outflux of the system (k_{14}) should be chosen according to experimental conditions. If these values were multiplied by 0.5 or 2 as well, the effect would be too drastic and lead to non-oscillatory kinetics (not shown). The initial steady state concentration of oxygen is the calculated value for either 18 or 38 °C, respectively.

3.3. Multiplication by 0.5

In Fig. 3, the values of the rate constants have been multiplied by 0.5, one by one, successively while the other rate constants were kept unchanged. The initial steady state concentration of oxygen was set at the extrapolated value for 18 °C (28−10 °C). In Fig. 3a, the *x*-axis indicates the rate constant that was multiplied by 0.5 and the *y*-axis the deviation from a control simulation. The period varies depending on the rate constant being changed. Halving the rate constant k_1 diminishes the period by 9% as compared to the control simulation. This is due to a diminution of the substrate influx and thus a reduced duration of the increase phase of an oscillation. Halving of k_2 causes a nearly unchanged period as the peroxidasic cycle will be slowed down. The period is increased if k_3 or k_4 is halved (by 21 and 11%, respectively). The period prolongation is even more pronounced (43%) when the production of the key radical superoxide in reaction R_5 is slowed down. Superoxide is involved in the peroxidasic cycle as well as in the formation of coIII. A slower formation of coIII, which is an important enzyme intermediate for the oscillatory system, in reaction R_6 increases the period by 14%. Halving of k_7 diminishes the dismutation of superoxide; however, the period becomes almost unchanged. Reaction

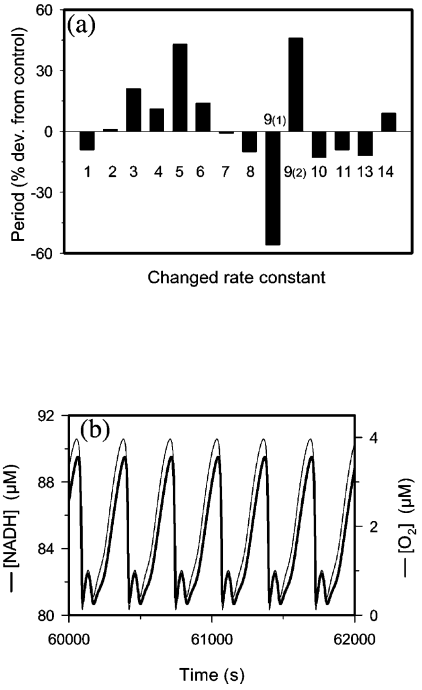

Fig. 3. Multiplication of each rate constant by 0.5 one by one while the values of the other rate constants are kept unchanged. The steady state concentration of oxygen is set at its value at 18 °C. For a control simulation where this is the only value changed, the period is 172 s. (a) The rate constant that has been changed is indicated on the *x*-axis, and the deviation of the resulting period from the control simulation is shown in percentage on the *y*-axis. (b) Time series for NADH and oxygen when k_9 is multiplied by 0.5. In this case mixed-mode oscillations, rather than simple oscillations, appear. They consist of a small-amplitude oscillation 9(1) and a large-amplitude oscillation 9(2).

R_8 is the decomposition of coIII. Halving of k_8 will liberate NAD$^\bullet$ radicals for use in the peroxidasic cycle for substrate consumption; the period is reduced by 10%. Halving of k_9, removal of NAD$^\bullet$ radicals from the system, leads to mixed-mode oscillations (Fig. 3b), with one small-amplitude oscillation alternating with one large-amplitude oscillation. Their period length will be considered as being the time from minimum to minimum. Using this definition, their periods are 56% shorter and 47% longer, respectively, than the control value. Lowering k_{10} leads to a liberation of NAD$^\bullet$ radicals for reaction with oxygen (R_5) and the period decreases (13%). A

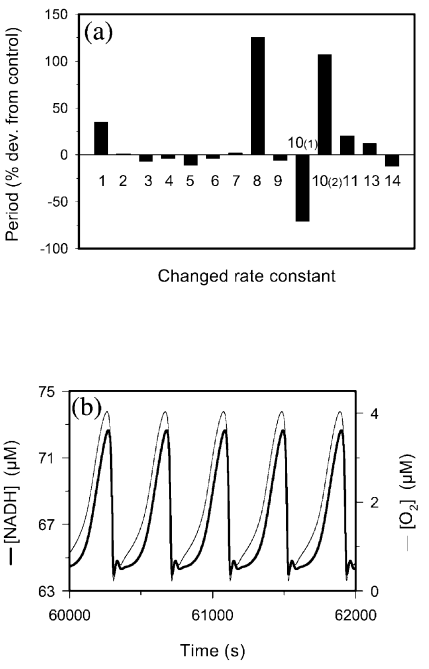

Fig. 4. Multiplication of each rate constant by 2 one by one while the values of the other rate constants are kept unchanged. The steady state concentration of oxygen is set at its value at 38 °C. For a control simulation where this is the only value changed, the period is 173 s. (a) The rate constant that has been changed is indicated on the *x*-axis, and the deviation in the resulting period from the control simulation is shown in percentage on the *y*-axis. (b) Time series for NADH and oxygen when k_{10} is multiplied by 2. In this case mixed-mode oscillations, rather than simple oscillations, appear. They consist of a small-amplitude oscillation 10(1) and a large-amplitude oscillation 10(2).

multiplication of k_{11} by 0.5 results in a 9% shorter period as oxygen instead of being incorporated in coIII will form superoxide. A diminution of the oxygen supply (k_{13}) results in a 12% shorter period as the mounting phase of the period will decrease, while a decrease of the oxygen efflux (k_{14}) results in a 9% longer period.

3.4. Multiplication by 2

In Fig. 4 the values of the rate constants have been multiplied by 2, one by one, successively while the other rate constants were kept unchanged. The initial steady state concentration of oxygen was set at the extrapolated value for 38 °C (28+10 °C). In Fig. 4a, the *x*-axis indicates the rate constant that was multiplied by 2 and the *y*-axis the deviation from a control simulation. Here, it is the doubling of k_{10}, and not k_9, that results in mixed-mode oscillations (Fig. 4b). Generally, the deviation from the control simulation is in the direction opposite to the direction in the case of multiplication by 0.5. An exception is k_2, but the deviation is within the error range. For some rate constants the deviation was much larger than by multiplication of that same constant by 0.5. Thus, with k_1 multiplied by 2, the increase in period is 35%, as compared to a 9% decrease for multiplication by 0.5. With k_8 multiplied by 2, the increase in period is 126%, as compared to a 10% decrease for multiplication by 0.5. And with k_{10} multiplied by 2, the first period is 73% shorter and the second period 110% longer, respectively, than the control period, while the period for k_{10} multiplied by 0.5 is 13% shorter than the control value.

3.5. Progressive multiplication of all constants by one and the same factor

The effect of multiplying all constants by one and the same factor, from 0.5 (18 °C) to 2 (38 °C), was investigated. Fig. 5a summarizes the periods as a function of the multiplication factor. When the multiplication factor (the 'temperature') is increased, there are intervals where the period increases (0.5–1.355; 18–31.75 °C), decreases (1.425–1.8; 32.25–36 °C), or is constant (1.85–2; 36.5–38 °C). Q_{10} values for four different intervals are listed in Table 2. It is seen that there are regions with Q_{10} higher than 1, approximately 1, and lower than 1.

Simple oscillations were observed between factors 0.5–1.355. Fig. 5b shows time series when using factor 0.9. Using factor 1.4 (Fig. 5c), two periods of equal length but different amplitude were found. For the following factors up to factor 2, mixed-mode oscillations with periods consisting of one small-amplitude oscillation and one large-amplitude oscillation were observed. Time series for a simulation using factor 1.9 is shown in Fig. 5d. The duration of these two sections of the total period is shown for the substrates as a function of

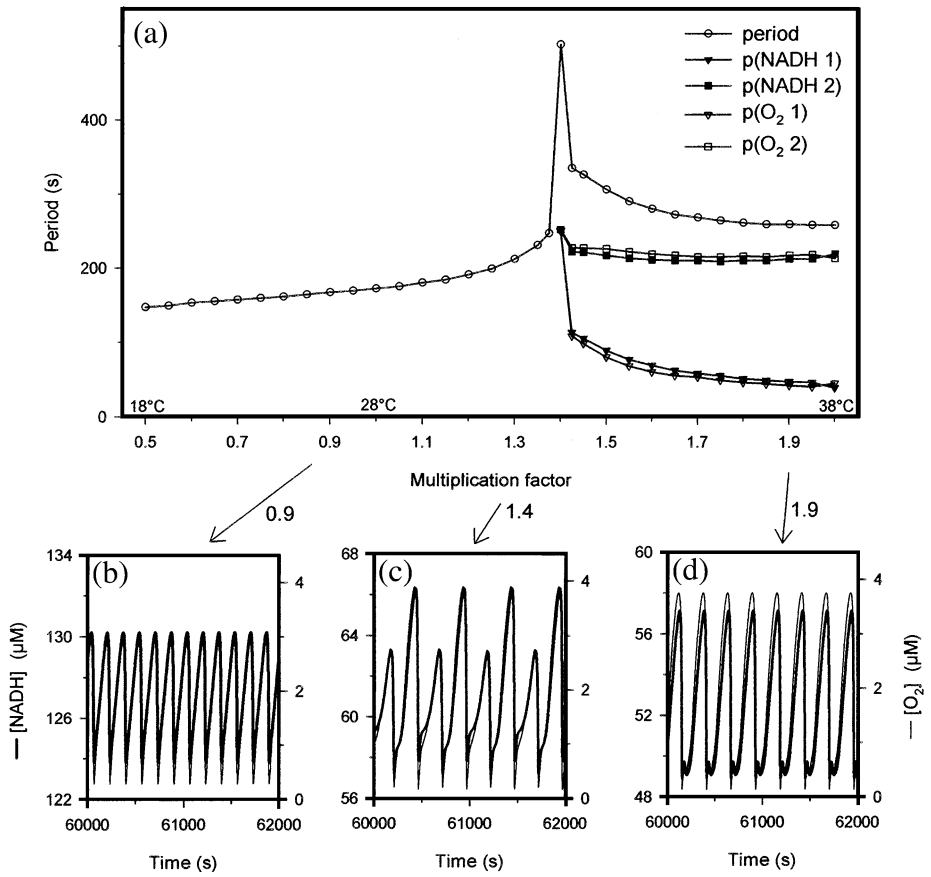

Fig. 5. Progressive multiplication of all rate constants by the same factor. (a) The period (○) is plotted against the multiplication factor. Above factor 1.4 the periods consist of a small-amplitude oscillation (▼▽) and a large-amplitude oscillation (■□). Below are time series for NADH and oxygen when all rate constants are multiplied by 0.9 (b), 1.4 (c), or 1.9 (d).

multiplication factor for the interval 1.4–2 in Fig. 5a.

The same result was obtained with the two integration methods Rosenbrock and Auto-stepsize (not shown). As a further verification of the result, simulations were performed based on the parameter values of Bronnikova et al. [16], using the multiplication factors 0.5, 1, 1.5 and 2. As for k_{13}, k_{14}, and oxygen steady state concentrations, a conversion factor was calculated for the values chosen for this study and applied to these data. These parameter values, together with the resulting

Table 2
Q_{10} values for different multiplication factor intervals (compare Fig. 5)

Multiplication factor interval	Temperature interval (°C)	Temperature difference (°C)	Q_{10} (from frequency)
0.5–1	18–28	10	0.85
0.7–1.355	22–31.75	9.75	0.66
1.425–1.8	32.25–36	3.75	1.91
1.85–2	36.5–38	1.5	1.03

Table 3
Simulations based on parameter values used by Bronnikova et al. [16]

Multiplication factor	Period (NADH) (s)	Period (oxygen) (s)	k_{13} ($\mu M\ s^{-1}$)	k_{14} (s^{-1})	$[O_2]_0$ (μM)
0.5	97	97	0.06	0.002949	19
1	96	97	0.0624	0.00373	16.7
1.5	167 (42+125)	166 (41+125)	0.06359	0.00412	15.24
2	198 (29+169)	198 (30+168)	0.06478	0.00451	13.78

substrate periods, are listed in Table 3. Again, an increase of multiplication factor results in an increased period in the interval from 0.5 to 2. Multiplication factors 1.5 and 2 give rise to mixed-mode oscillations. In the table, the value of the period for the total oscillation is followed by an indication of the time lengths of its small-amplitude oscillation and its large-amplitude oscillation in brackets.

4. Discussion

The 'temperature' sensitivity of each individual rate constant was investigated in the way of its multiplication by either 0.5 or 2, the other constants being kept unchanged. The overall result is similar to the results obtained by Leloup and Goldbeter [28]: depending on which rate constant being considered, the conclusion was: (1) the effect on period length is either positive or negative, (2) the magnitude of the change in period length differs, and (3) multiplication by 0.5 or by 2 does not in all cases have opposite effects. As for (3), here, not only the magnitude of the change of period length for a given rate constant differed, but also the dynamics: multiplication of k_9 by 0.5 or k_{10} by 2 caused the occurrence of mixed-mode oscillations. For all other cases, only simple oscillations were observed.

The change of one rate constant in the reaction network will dislocate the balance of the whole network in a way determined by which constant has been changed. This can explain why the effect of a given stimulus can differ depending on the rate constant being changed.

Whereas progressive multiplication of all constants by one and the same factor in the model of the circadian rhythmicity of the PER protein showed nearly full temperature compensation [28], the PO system showed a more complex behavior. Depending on the 'temperature' region, an increase in 'temperature' results in either a longer, shorter, or almost constant period (Fig. 5a).

It may seem surprising that the period can become longer as temperature increases, because the opposite effect normally is seen in the case of elementary biochemical reactions. With increased temperature the frequency of molecular collisions will increase, making reactions more likely to occur and thus increases the reaction rate. If the overall reaction rate of an oscillatory system accelerates, then the increasing phase of an oscillation will be shorter before substrate is consumed and a new minimum is reached. The result would be a shorter period (i.e. a higher frequency). That such a linear response to temperature is not seen here is due to the complexity of the present non-linear system, which has feedback loops and rate constants responding in opposite directions to the same temperature change. The system is over-compensated in this case, corresponding to a Q_{10} value below 1. Examples of over-compensation have been found in biological systems [40–43].

The Q_{10} values corresponding to the periods vary from $Q_{10}=0.7$ (over-compensation) via $Q_{10}=1$ (temperature compensation) to $Q_{10}=1.9$ (no temperature compensation) for the intervals chosen in Table 3, i.e. there is no linear correlation between multiplication factor ('temperature') and period, despite the fact that the mutual relationship between most rate constants remains the same. However, the relationship between these constants and the substrate concentrations as well as the substrate input/output changes. The inflow of NADH (k_{12}) was kept constant. For the hypothetical temperature in question, the initial aqueous

oxygen concentration was chosen according to extrapolated values and the oxygen mass transport constants (k_{13} and k_{14}) from experimental observations. The changed relationship between these parameters and rate constants k_1–k_{11}, which were multiplied by a different, common factor, dislocate the balance in the reaction network, which may change the resulting period.

Under experimental conditions, not all rate constants for the enzymatically catalyzed reactions will increase by the same factor. Their temperature sensitivity depends on the activation energy needed for the given partial reaction to occur (which has not been taken into account here). In addition to the enzyme-catalyzed reactions, the reaction network consists of several non-enzymatic reactions [4], of which some are included in the model (R_1, R_5, R_7, R_9, R_{12}, R_{13}, R_{14}), and a temperature-dependent steady state oxygen concentration. Their temperature dependency will differ from the enzyme-catalyzed reactions.

Thus, the interrelationship between the rate constants will change when temperature changes, and the same reaction may have different Q_{10} values depending on the temperature region considered.

Theoretically therefore, it may be possible for the very same reaction to exhibit both temperature compensation (to a varying extent), temperature dependency, and over-compensation.

The region around factor 1.4 was found to be critical. The biggest changes in period were found around this value, with a steep increase before and a steep decrease after factor 1.4. If such an unstable parameter region was found experimentally, the outcome would be quite different depending on which side it was approached from, leading to either over-compensation or only partial compensation.

Temperature compensation is considered to be a characteristic of circadian rhythms, while ultradian oscillators are considered as being temperature dependent (e.g. [19]). However, the influence of this environmental parameter on oscillators is more complicated as such. Thus, there are examples of temperature dependent circadian oscillators [44–47] found in environments of stable temperature, making the ability of temperature compensation unnecessary. Further evidence that temperature compensation is not a prerequisite for circadian rhythmicity to occur is the fact that rhythmicity persists in *Neurospora crassa* despite a disruption of the temperature compensation mechanism [48].

Ultradian oscillators are generally temperature dependent. An example is the oscillations in intracellular calcium concentration [49]. The temperature dependency was confirmed [50] using a model developed by Goldbeter et al. [51]. However, ultradian oscillators may be thermo-compensated as well [20–23].

Interestingly, the same pulvinar cells in bean (*Phaseolus vulgaris* L.) induce thermo-compensated circadian leaf movements as well as temperature dependent ultradian leaf movements [52].

Temperature compensation is not a phenomenon restricted to biological systems. It was observed in a chemical system involving iodine [53] and in the oscillatory hydrogenperoxide–thiosulfate system [54].

On the other hand the Belousov–Zhabotinsky (BZ) reaction, which is a classical chemical model system for non-linear phenomena, generally is temperature dependent. In the case of a continuous-flow stirred tank reactor system the reaction shows partial temperature compensation, though [55]. By finding a balance between reaction rates influencing the period in opposite directions it was possible to obtain temperature compensation in a simulation of the reaction [26].

Thus, for any model of an oscillatory system, temperature compensation can be achieved by the establishment of an antagonistic balance between rate expressions leading to a larger period and expressions leading to a smaller period [25]. In this manner, temperature compensation can be achieved in the Brusselator model [24], the Oregonator model [26], the Goodwin model [27], and in the present work.

Acknowledgments

The authors thank L.F. Olsen for useful suggestions concerning the numerical computations.

References

[1] B. Dunford, Heme Peroxidases, Wiley, New York, 1999.
[2] T. Akazawa, E.E. Conn, The oxidation of reduced pyridine nucleotides by peroxidase, J. Biol. Chem. 232 (1958) 403–415.

[3] R. Larter, L.F. Olsen, C.G. Steinmetz, T. Geest, in: R.J. Field, L. Györgyi (Eds.), Chaos in Chemistry and Biochemistry, World Scientific Publishers, London, 1993.
[4] A. Scheeline, D.L. Olson, E.P. Williksen, G.A. Horras, The peroxidase–oxidase reaction and its constituent chemistries, Chem. Rev. 97 (1997) 739–756.
[5] G.G. Gross, C. Janse, E.F. Elstner, Involvement of malate, monophenols, and the superoxide radical in hydrogen peroxide formation by isolated cell walls from horseradish *Armoracia lapathifolia*, Planta 136 (1977) 271–276.
[6] M.J.B. Hauser, U. Kummer, A.Z. Larsen, L.F. Olsen, Oscillatory dynamics protect enzymes and possibly cells against toxic substances, Faraday Disc. 120 (2001) 215–227.
[7] I. Yamazaki, K. Yokota, Oxidation states of peroxidase, Mol. Cell. Biochem. 2 (1973) 39–52.
[8] B.D. Aguda, L.-L. Hofmann Frisch, L.F. Olsen, Experimental evidence of the coexistence of oscillatory and steady states in the peroxidase–oxidase reaction, J. Am. Chem. Soc. 112 (1990) 6652–6656.
[9] M.J.B. Hauser, L.F. Olsen, Mixed-mode oscillations and homoclinic chaos in an enzyme reaction, J. Chem. Soc. Faraday Trans. 92 (1996) 2857–2863.
[10] L.F. Olsen, H. Degn, Chaos in an enzyme reaction, Nature 267 (1977) 177–178.
[11] T. Geest, L.F. Olsen, C.G. Steinmetz, R. Larter, W.M. Schaffer, Period-doubling bifurcations and chaos in an enzyme reaction, J. Phys. Chem. 96 (1992) 5678–5680.
[12] L.F. Olsen, An enzyme reaction with a strange attractor, Phys. Lett. 94A (1983) 454–457.
[13] K. Yokota, I. Yamazaki, Analysis and computer simulation of aerobic oxidation of reduced nicotinamide adenine dinucleotide catalyzed by horseradish peroxidase, Biochemistry 16 (1977) 1913–1920.
[14] B.D. Aguda, R. Larter, Periodic-chaotic sequences in a detailed mechanism of the peroxidase–oxidase reaction, J. Am. Chem. Soc. 113 (1991) 7913–7916.
[15] D.L. Olson, E.P. Williksen, A. Scheeline, An experimentally based model of the peroxidase-NADH biochemical oscillator: an enzyme-mediated chemical switch, J. Am. Chem. Soc. 117 (1995) 2–15.
[16] T.V. Bronnikova, V.R. Fed'kina, W.M. Schaffer, L.F. Olsen, Period-doubling bifurcations and chaos in a detailed model of the peroxidase–oxidase reaction, J. Phys. Chem. 99 (1995) 9309–9312.
[17] D.L. Olson, A. Scheeline, The peroxidase-NADH biochemical oscillator: experimental system, control variables, and oxygen mass transport, Anal. Chim. Acta 283 (1993) 703–707.
[18] K. Valeur, L.F. Olsen, Kinetic studies of the oscillatory dynamics in the peroxidase–oxidase reaction catalyzed by four different peroxidases, Biochim. Biophys. Acta 1289 (1996) 377–384.
[19] E. Bünning, The Physiological Clock, Springer, New York, Heidelberg, Berlin, 1973.
[20] I. Balzer, U. Neuhaus-Steinmetz, R. Hardeland, Temperature compensation in an ultradian rhythm of tyrosine aminotransferase activity in *Euglena gracilis* Klebs, Experimentia 45 (1989) 476–477.
[21] F. Kippert, D. Lloyd, A temperature-compensated ultradian clock ticks in *Schizosaccharomyces pombe*, Microbiology 141 (1995) 883–890.
[22] F. Kippert, A temperature-compensated clock of *Tetrahymena*: oscillations in respiratory activity and cell division, Chronobiol. Int. 13 (1996) 1–13.
[23] D.J. Morré, D.M. Morré, NADH oxidase activity of soybean plasma membranes oscillates with a temperature compensated period of 24 min, Plant J. 16 (1998) 277–284.
[24] P. Ruoff, Introducing temperature-compensation in any reaction kinetic oscillator model, J. Interdiscipl. Cycle Res. 23 (1992) 92–99.
[25] P. Ruoff, General homeostasis in period- and temperature-compensated chemical clock mutants formed by random selection conditions, Naturwissenschaften 81 (1994) 456–459.
[26] P. Ruoff, Antagonistic balance in the Oregonator: about the possibility of temperature-compensation in the Belousov–Zhabotinsky reaction, Physica D 84 (1995) 204–211.
[27] P. Ruoff, L. Rensing, The temperature-compensated Goodwin oscillator simulates many circadian clock properties, J. Theor. Biol. 179 (1996) 275–285.
[28] J.-C. Leloup, A. Goldbeter, Temperature compensation of circadian rhythms: control of the period in a model for circadian oscillations of the PER protein in *Drosophila*, Chronobiol. Int. 14 (1997) 511–520.
[29] P. Sevcik, H.B. Dunford, Kinetics of the oxidation of NADH by methylene blue in a closed system, J. Phys. Chem. 95 (1991) 2411–2415.
[30] A.C. Møller, L.F. Olsen, Perturbations of simple oscillations and complex dynamics in the peroxidase–oxidase reaction using magnetic fields, J. Phys. Chem. B 104 (2000) 140–146.
[31] E.S. Kirkor, A. Scheeline, M.J.B. Hauser, Principal component analysis of dynamical features in the peroxidase–oxidase reaction, Anal. Chem. 72 (2000) 1381–1388.
[32] E.J. Land, A.J. Swallow, One-electron reactions in biochemical systems as studied by pulse radiolysis. I. Nicotine-adenine dinucleotide and related compounds, Biochim. Biophys. Acta 162 (1968) 327–337.
[33] B.H.J. Bielski, P.C. Chan, Studies on free and enzyme-bound nicotinamide adenine dinucleotide free radicals, J. Am. Chem. Soc. 102 (1980) 1713–1716.
[34] L.S. Clesceri, A.E. Greenberg, R.R. Trussel, Standard Methods for the Examination of Water and Wastewater, 19th ed., American Public Health Association, Washington, DC, 1995.
[35] Microelectrodes, Inc., MI-730 Micro-Oxygen Electrode, Operating Instructions.
[36] I.H. Segel, Enzyme Kinetics, Wiley, New York, 1975.

[37] A.C. Hindmarsh, LSODE and LSODI, two new initial value ordinary differential equation solvers, Signum Newslett. 15 (1980) 10–11.
[38] L.F. Olsen, A. Lunding, F.R. Lauritsen, M. Allegra, Melatonin activates the peroxidase–oxidase reaction and promotes oscillations, Biochem. Biophys. Res. Commun. 284 (2001) 1071–1076.
[39] M.J.B. Hauser, A. Lunding, L.F. Olsen, On the role of methylene blue in the oscillating peroxidase–oxidase reaction, Phys. Chem. Chem. Phys. 2 (2000) 1685–1692.
[40] V.F. Bühnemann, Das endodiurnal system der oedogoniumzelle. III. Uber den temperatureinfluβ, Z. Naturforsch. 10b (1955) 305–310.
[41] R. Hardeland, I. Balzer, Influences of temperature on circadian and ultradian rhythms, in: J. Beau, J.-F. Vibert (Eds.), Rhythmes Biologiques, Paris Polytechnica, Paris, 1993.
[42] J.W. Hastings, B.M. Sweeney, On the mechanism of temperature independence in a biological clock, Proc. Natl. Acad. Sci. USA 43 (1957) 804–811.
[43] M.W. Karakashian, H.G. Schweiger, Circadian properties of the rhythmic system in individual nucleated and enucleated cells of *Acetabularia mediterranea*, Exp. Cell Res. 97 (1976) 366–377.
[44] K.K. Nanda, K.C. Hamner, Effects of temperature, auxins, antiauxins and some other chemicals on the endogenous rhythm effecting photoperiodic response of Biloxi soybean, Planta 53 (1959) 53–68.
[45] L. Overland, Endogenous rhythm in opening and odor of flowers of *Cestrum nocturnum*, Am. J. Bot. 47 (1960) 378–382.
[46] H. Sylin-Roberts, W. Engelmann, K.G. Grell, *Thalassomyxa australis* rhythmicity. I. Temperature dependence, J. Interdiscpl. Cycle Res. 17 (1986) 181–187.
[47] E. van Praag, R. degli Agosti, R. Bachofen, Rhythmic activity of uptake hydrogenase in the prokaryote *Rhodospirillum rubrum*, J. Biol. Rhythms 15 (2000) 1–7.
[48] J.J. Loros, J.F. Feldman, Loss of temperature compensation of circadian period length in the frq-9 mutant of *Neurospora crassa*, J. Biol. Rhythms 1 (1986) 187–198.
[49] R.J. Hajjar, J.V. Bonventre, Oscillations of intracellular calcium induced by vasopressin in individual fura-2-loaded mesangial cells, J. Biol. Chem. 266 (1991) 21589–21594.
[50] R. degli Agosti, Temperature effect on the frequency of simulated intracellular calcium oscillations, in: H. Greppin, M. Bonzon, R. degli Agosti (Eds.), Some Physicochemical and Mathematical Tools for Understanding of Living Systems, University of Geneva, Geneva, 1993.
[51] A. Goldbeter, G. Dupont, M.J. Berridge, Minimal model for signal-induced Ca^{2+} oscillations and for their frequency encoding through protein phosphorylation, Proc. Natl. Acad. Sci. USA 87 (1990) 1461–1465.
[52] B. Millet, A.-M. Botton, C. Hayoum, W.L. Koukkari, An experimental analysis and comparison of three rhythms of movements in bean (*Phaseolus vulgaris* L.), Chronobiol. Int. 5 (1988) 187–193.
[53] A. Skrabal, Vorlesungsversuch zur demonstration eines falles der abnahme der reaktionsgeschwindigkeit mit der temperatur, Z. Elektrochemie 19/20 (1915) 461–463.
[54] G. Rábai, I. Hanazaki, Temperature compensation in the oscillatory hydrogen peroxide-thiosulfate-sulfite flow system, Chem. Commun. (1999) 1965–1966.
[55] G. Nagy, E. Körös, N. Oftedal, K. Tjelflaat, P. Ruoff, Effect of temperature in cerium ion catalyzed bromate driven oscillators, Chem. Phys. Lett. 250 (1996) 255–260.